## LITERATURE CITED

1. Davies, R. J., *Phil. Mag.*, **15**, 489 (1933).
2. Glueckauf, E., *Paper SWD/1*, First Intern. Symp. Water Desalination, Washington, D. C. (Oct., 1965).
3. Govindan, T. S., and S. Sourirajan, *Ind. Eng. Chem. Process Design Develop.*, **5**, 422 (1966).
4. Kolthoff, I. M., and J. J. Lingane, "Polarography," Vol. 1, Interscience, New York (1952).
5. Lewis, G. N., and M. Randall, "Thermodynamics," 2 ed., revised by K. S. Pitzer, and L. Brewer, p. 324, McGraw-Hill, New York (1961).
6. Lin, C. S., E. B. Denton, H. S. Gaskill, and G. L. Putnam, *Ind. Eng. Chem.*, **43**, 2136 (1951).
7. Loeb, Sidney, and S. Sourirajan, *Advan. Chem. Ser. No. 38*, 117 (1963).
8. Lonsdale, H. K., U. Merten, and R. L. Riley, *J. Appl. Polymer Sci.*, **9**, 1341 (1962).
9. Öholm, L. W., *Finska Kemistsamfundets Medd.*, **45**, 71 (1936); **47**, 115 (1938).
10. Reiss, L. P., and T. J. Hanratty, *A.I.Ch.E. J.*, **8**, 245 (1962).
11. Robinson, R. A., and R. H. Stokes, "Electrolytes Solutions," Butterworths, London (1959).
12. Sourirajan, S., *Ind. Eng. Chem. Fundamentals*, **3**, 206 (1964).
13. ———, *J. Appl. Chem.*, **14**, 506 (1964).
14. ———, and T. S. Govindan, *Paper SWD/41*, First Intern. Symp. Water Desalination, Washington, D. C. (Oct., 1965).



*Manuscript received June 17, 1966; revision received September 26, 1966; paper accepted September 26, 1966.*


# An Investigation of Solids Distribution, Mixing, and Contacting Characteristics of Gas-Solid Fluidized Beds


**M. M. EL HALWAGI and ALBERT GOMEZPLATA**

**University of Maryland, College Park, Maryland**



**This two-part series describes an integrated experimental investigation. The first part is concerned with the determination of axial and radial solids concentration profiles at different superficial gas velocities for three columns having I.D. of 2.5, 6.5, and 9.5 in. respectively. The second part is concerned with steady state point source gas tracer experiments carried out in the 9.5-in. column and in which the tracer concentration was measured at different radial positions above and below the injection source at various gas velocities Both parts are complimentary to each other for describing the internal flow behavior of the gas-solid fluidized system.**


## PART I. STUDY OF SOLID CONCENTRATION PROFILES IN A GAS-SOLID FLUIDIZED BED

Despite the widespread use of gas-solid fluidized beds, many of their fundamentals are still poorly understood. In recent years, it has been realized that in order to achieve the desired understanding of the phenomenon of gas-solid contact in fluidized systems, the approach of determining the overall characteristics of the system has to be replaced by a more fundamental approach based on the measurement of the variation of the properties from point to point within the system. Such an approach was followed throughout this work.

The first part of this investigation was concerned with the study of time-averaged solids distribution of different diameter fluidized beds with the gamma ray attenuation


M. M. El Halwagi is with the National Council of Research, Cairo, Egypt.

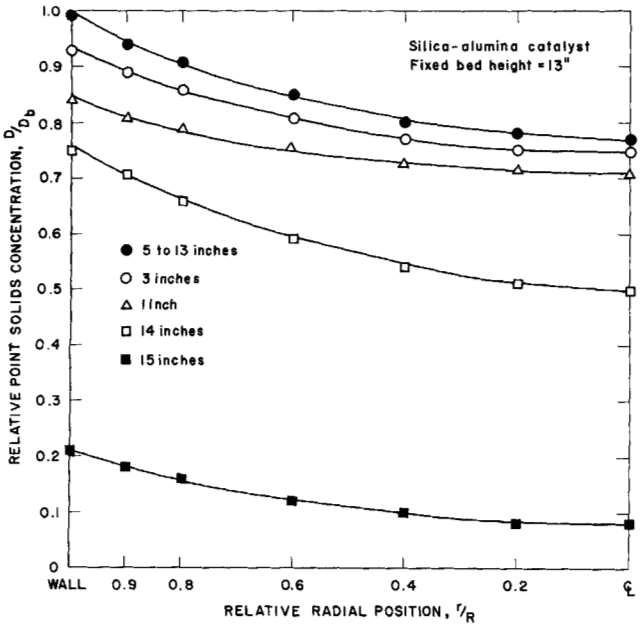


Fig. 1. Radial concentration profiles of solids at different heights (6.5-in. column, 0.3 ft./sec., porous plate).

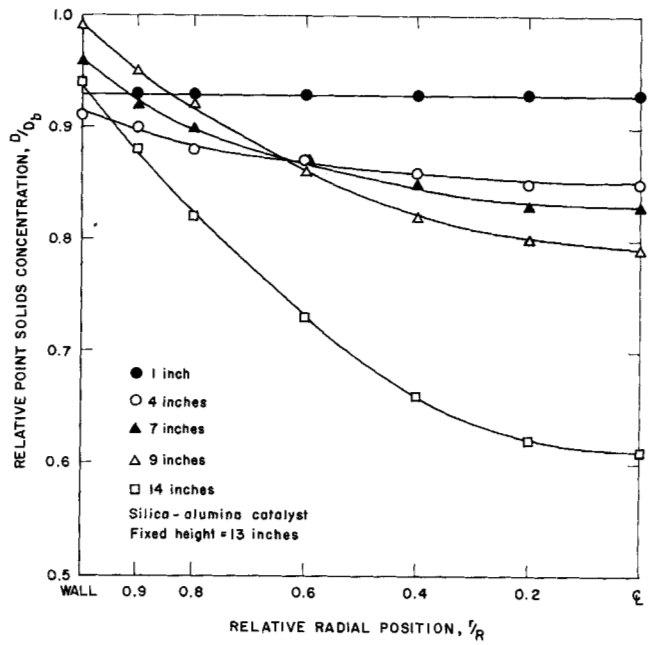


Fig. 3. Radial concentration profiles of solids at different heights (6.5-in. column, 0.3 ft./sec., multiorifice plate).

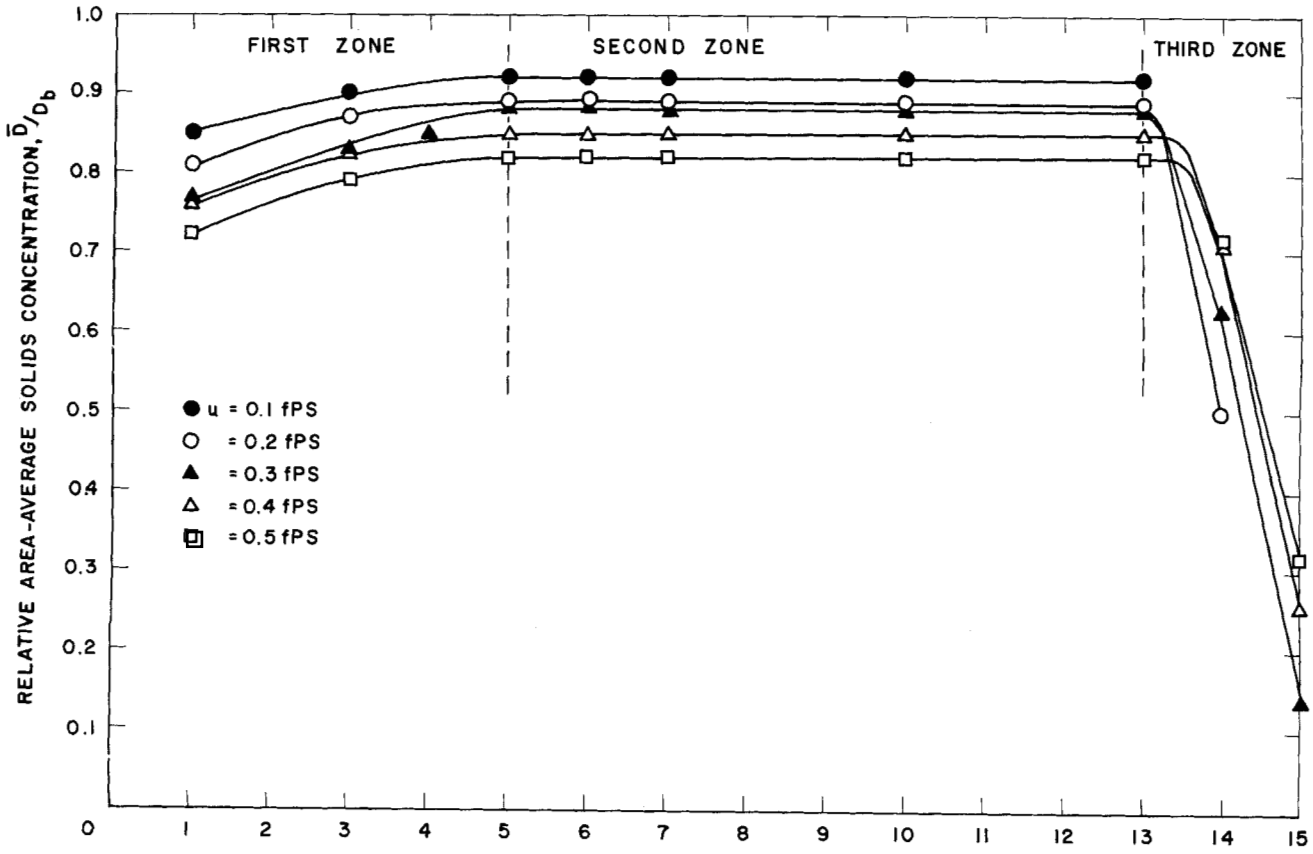


Fig. 2. Variation of area-averaged solids concentration with height at different gas velocities (6.5-in. column, fixed bed height 13 in., porous plate).

technique used. At the conclusion of this phase of work it appeared that the results of this part, combined with further information from suitable gas tracer experiments, and when interpreted in terms of the two-phase flow concept, would lead to the evolution of a truer picture of the internal flow behavior of the system and to an estimate of the extent of gas back-mixing and the effectiveness of contact between the two phases. Consequently, steady state gas tracer experiments were performed in the second part to evaluate this possibility.

## PREVIOUS WORK

Several workers have studied fluid bed density and its variation with system conditions. Matheson et al. (*22*) calculated the bed density from pressure drop measurements over a finite height of the bed, and the density was found to decrease with increased gas velocity. Grohse (*17*) measured bed densities by means of an x-ray absorption technique using three different distributors: a porous plate, a multiorifice plate, and a screen. For the porous plate the density was found to be remarkably constant over the entire bed, while for the other plates the density pattern was quite irregular, exhibiting the highest density at the bottom of the bed.

Bartholomew and Casagrande (*5*) and Hunt et al. (*19*) used a gamma ray absorption technique to measure radial solids distribution at one elevation of vertical catalyst risers in fluid cracking units. In both studies solids concentration was generally found to increase from the center radially to the wall.

Bakker and Heertjes (*2, 3*), using a capacitive probe technique, measured the time-averaged porosity distributions in a small (9-cm. diameter) gas-fluidized bed, and they identified three regions: the sieve or entry section of decreasing porosity from the bottom of the bed, a middle zone porosity extending to the prefluidized bed height, and the top zone of continuously increasing porosity. They pointed out, however, that the capacitive method they used has the disadvantage of introducing an alien body in the bed which may thus disturb the internal flow behavior.

Fan et al. (*11*) measured the axial average density profiles using a gamma ray attenuation technique, and reported two distinct density zones: a relatively constant zone in the lower portion of the column and a rapidly decreasing zone at the top portion of the column. They empirically correlated their average density results in the lower portion of the column with the gas velocity and solids particle size.

Grek and Kisel'nikov (*16*) determined axial porosity profiles using an acoustic method and reported results similar to those of Bakker and Heertjes (*2*). The authors were mainly concerned with development and validity of the method (which is based on the absorption of sound waves), and therefore only outlined a few representative results.

## THE GAMMA RAY ATTENUATION TECHNIQUE FOR MEASURING SOLIDS DISTRIBUTION

The gamma ray attenuation technique has the important advantage of measuring phase concentrations externally without disturbing the internal flow behavior of the system.

For a gas-solid fluidized system it has been shown (*5*) that if the absorption of radiation by the gas is neglected, the mean solids concentration $D_m$ over a chosen path of length $L$ can be calculated and is usually expressed as a ratio of the bulk density $D_b$.

Once the mean path concentrations are determined over a large number of paths covering the cross section of the bed as completely as possible, solids point distribution can be determined by assuming a polynomial function for the point concentration distribution, and then determining the polynomial coefficients from the measured mean path concentrations (*10*). The calculations were made with an IBM 7094 computer.

## EQUIPMENT AND MATERIALS

### Fluidization Equipment

The fluidization assembly consisted of a vertical Plexiglas cylindrical column provided with a gas distributor and connected to a polyethylene funnel used for air inlet, a source of air, a rotameter, and a pressure gauge for measuring the air flow rate and its pressure.

Three columns with I.D. of 3.5, 6.5, and 9.5 in. were used in conjunction with the solids distribution measurements. Porous plate distributors were utilized in most of the work. An additional multiorifice plate was used with the 6.5-in. column. To ensure uniform air distribution with this multiorifice plate, it was designed such that the pressure drop through it, at the lowest velocity used (0.1 ft./sec.), was approximately equal to that through the porous plate at the same velocity.

### Gamma Ray Equipment

The equipment used for measuring solids concentration by the gamma ray attenuation technique consisted of a 5-mc. $Cs^{137}$ source, a collimated scintillation detector, a single-channel gamma ray spectrometer, and a positioning table which could be moved vertically and on which positioning tracks for both the source and the detector were made.

### Materials

The powder used in most of the experiments was silica-alumina cracking catalyst with a settled bulk density of 42 lb./cu. ft. and a minimum fluidization velocity of about 0.02 ft./sec. A few solids concentration profiles were obtained for an iron oxide catalyst with a settled bulk density of 170 lb./cu. ft. and a minimum fluidization velocity of about 0.03 ft./sec.

## EXPERIMENTAL MEASUREMENTS AND PROCEDURE

The base, window, and the operating voltage of the single-channel analyzer were adjusted to peak counting to eliminate errors due to scatter radiation. Experiments indicated axial symmetry, and therefore measurements were only obtained for half the column at the relative radial positions ($r/R$) of: 0, 0.2, 0.4, 0.6, 0.8, and 0.9, and at various levels above the distributor.

Four count rate measurements were necessary to determine the mean solids concentration over each path: a reference count rate measurement with an empty column, an empty column count rate, a full nonfluidized bed count rate, and a fluidized bed count rate. The reproducibility of the data was found to be within $\pm 3\%$.

## RESULTS AND DISCUSSION

Typical time average solids concentration profiles are shown in Figure 1 for the 6.5-in. column at an air velocity of 0.3 ft./sec. and at different heights with porous plate distributor used. Similar profiles were obtained for all the columns under the investigated operating conditions. The shown radial profiles exhibit the highest concentration at the wall and the lowest at the center, and they tend to be flatter near the bed distributor. Examination of the axial variations indicates the presence of three distinct axial zones which were reported previously by Bakker and Heertjes (*2*): the first region is adjacent to the bed distributor, a following fully developed region exhibiting constant solids concentrations and reaching to about the initial fixed bed height, and a third region extending to the top of the bed and in which solids concentration decreases sharply with height. These regions are indicated in Figure 2 for runs made with a 6.5-in. column with the use of a porous plate.

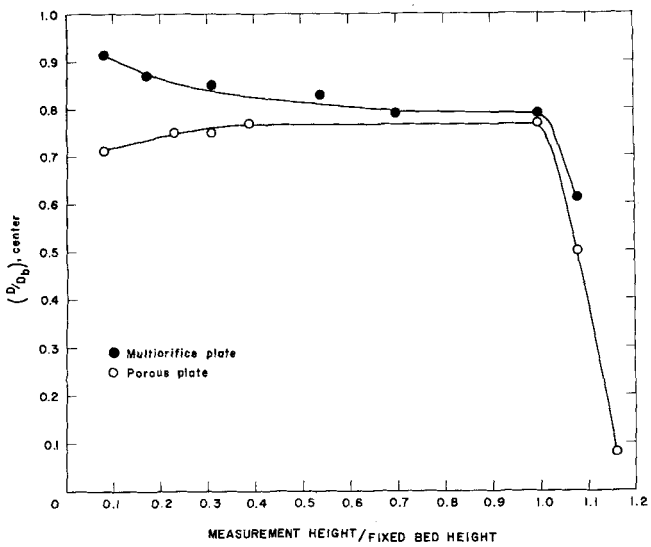


**Fig. 4. Comparison of the axial profiles at the center for the porous and multiorifice distributors (6.5-in. column, 0.3 ft./sec.).**

The characteristics of the first region seem to be dependent on the type of the gas distributor used. This may be demonstrated by comparing the solids concentration profiles in this region using a multiorifice plate to those obtained with a porous plate under similar conditions (Figures 1, 3, and 4).

These differences are probably the result of the initial size and velocity of the bubbles as they form at the distributor. A porous plate is known to be the best available kind of distributor from the standpoint of the small size of bubbles formed which leads to a smooth and good expansion. Bubbles forming from the multiorifice plate, on the other hand, are probably larger in size and faster, which would not result in as good an expansion close to the plate, and therefore the first few inches would appear not to be completely fluidized and merely serve as an extension to the distributor.

The second fully developed region seems to be a basic stable zone in gas-fluidized beds constituting a large portion of the solids mass in the bed, and consequently most of the attention in this work has been focused on its study. The characteristics of this region were found to be independent of the initial fixed bed height, which was varied from one to three column diameters. The effects of column diameter and gas velocity can be seen by examining Figure 5. Radial profiles were flatter with increasing bed diameter and decreasing air velocity. The existence of higher solids concentrations in the wall region supports the usually reported visual observation that solids flow down the wall and up the center, and it gives an indication that such a concentration profile will always persist even for very large column diameters. The decrease in solids average concentration in this region with increasing superficial air velocity is illustrated in Figure 6, and shows that it is independent of column diameter within the experimental accuracy.

Profiles obtained with an iron oxide catalyst used indicate that similar distribution patterns are valid for aggregatively fluidized beds. A few profiles were also obtained for an air-water two-phase system and show a similarity to a fluidized system.

The third region, which may be called the *dilute phase region*, results from elutriation of solid particles by the movement of the bubbles before breaking from the surface and thus will increase in size at higher gas velocities, as can be seen in Figure 2. Only a few indicative profiles

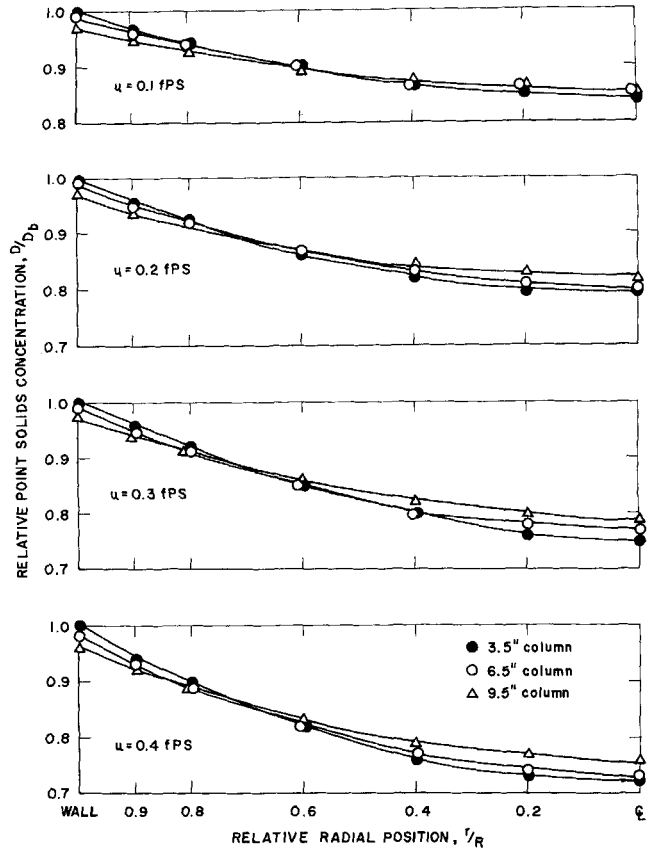


**Fig. 5. Radial solids concentration profiles in the fully developed region.**

were determined in this region because of the poor accuracy of the gamma ray attenuation technique in regions of low solids concentrations.

## A SIMPLIFIED MIXING LENGTH MODEL FOR PREDICTING SOLIDS DISTRIBUTION IN THE FULLY DEVELOPED REGION

A particulately fluidized bed is characterized by uniform solids distribution with no radial gradients. On the other hand, an aggregatively fluidized bed, as shown by the results of this work, exhibits considerable radial gradients, indicating a nonuniform bubble distribution. These concentration gradients are caused by the presence of gas

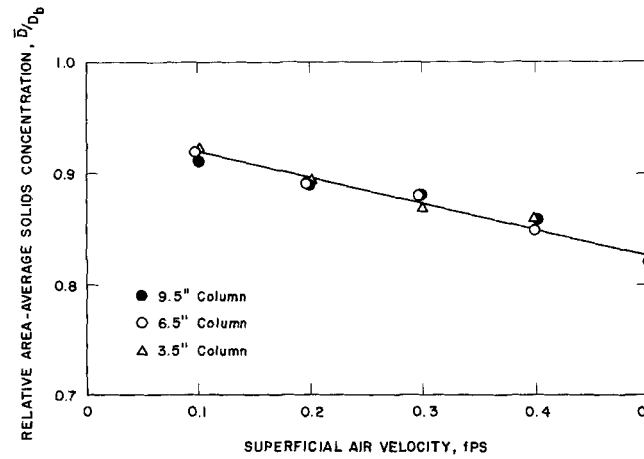


**Fig. 6. Variation of area-averaged solids concentration with gas velocity.**

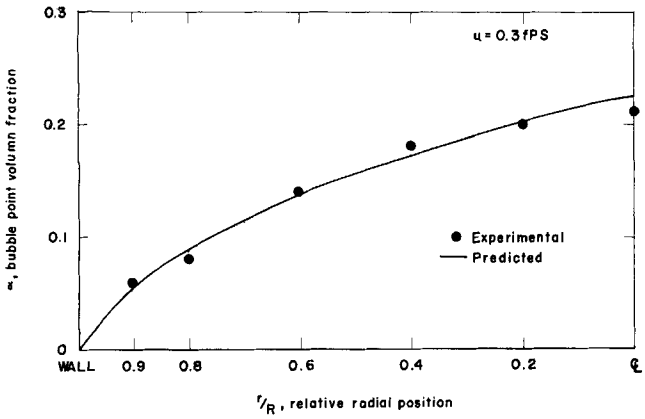


Fig. 7. Comparison of predicted vs. experimental bubble point volume fraction (9.5-in. column).

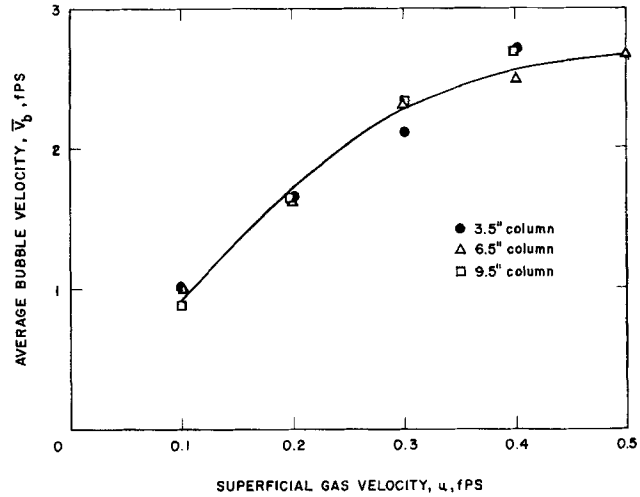


Fig. 8. Average bubble velocity in the fully developed region vs. superficial gas velocity.

bubbles, and consequently a reasonable correlation should be based on some sort of a simplified bubble model.

Recently much support has been given to the two-phase theory of fluidization and to the similarity between the behavior of large gas bubbles in liquids and bubbles in fluidized beds (*8*). Because of this similarity and because of the relative simplicity and reasonable success of the mixing length model in the prediction of density distribution in gas-liquid systems (*4, 21*), the model proposed here will be based on Prandtl mixing length theory and the treatment of the aggregatively fluidized bed as being composed of two constant density phases, namely, the bubble and dense phases.

### Model Formulation

If $\alpha$ is the local time-averaged bubble volume fraction, then the time-averaged point density of the two-phase mixture when the dense phase density is much larger than the gas is given by

$$D = D_b(1 - \alpha) \tag{1}$$

The instantaneous point density can vary from the dense phase density to the gas density, depending on whether a bubble is passing through this point at this instant. Accordingly it is assumed that the fluctuating density component $D'$ is directly proportional to the time-averaged point bubble volume fraction. If one further assumes that the Prandtl mixing length relation holds for the density fluctuations, then

$$D' = k_1 \alpha = l_D \frac{dD}{ds} = Ks \frac{dD}{ds} \tag{2}$$

Differentiating (1) and substituting into (2), one obtains

$$\frac{d\alpha}{\alpha} = N \frac{ds}{s}$$

where

$$N = \frac{k_1}{KD_B}$$

Integrating with $\alpha = \alpha_c$ at $s = 1$, we get

$$\frac{\alpha}{\alpha_c} = s^N \tag{3}$$

The exponent $N$ in Equation (3) was calculated by the least squares method for the three columns. The relative void fraction for a given column diameter can be characterized by a single value of $N$: 0.75 for the 3.5 in I.D., 0.60 for 6.5 in I.D., and 0.52 for 9.5 in I.D.

A typical comparison of experimental vs. predicted bubble volume fraction in the 9.5-in. column at a gas velocity of 0.3 ft./sec. is shown in Figure 7.

More extensive work is needed to investigate the effect of larger column diameters and different powders before a final comprehensive correlation is obtained.

## AVERAGE BUBBLE VELOCITIES AND EQUIVALENT DIAMETERS IN THE FULLY DEVELOPED REGION

Recent work on bubble motion and characteristics in gas-fluidized beds (*25* to *27*, *30*, *8*) has indicated that the average bubble velocity and diameter are two related and useful parameters in characterizing the internal flow behavior of the system. The average bubble velocity can be calculated directly from experimental data, whereas the average bubble diameter can only be determined indirectly from the calculated bubble velocity, utilizing a literature proposed relationship.

The average bubble velocity is given by

$$\overline{V}_b = (u - u_o)/\overline{\alpha}$$

Values of $\overline{V}_b$ were calculated and plotted in Figure 8 for the three columns at different gas velocities, and could be presented within the experimental accuracy by a single curve.

An expression for the absolute bubble rising velocity ($\overline{V}_b$) in terms of equivalent bubble diameter ($D_e$) is given

Table 1. Average Bubble Velocity and Equivalent Diameter in the Fully Developed Region

Solid used: Silica-alumina cracking catalyst
Distributors: Porous plates

| | Column diameter, in. | | | | | |
|---|---|---|---|---|---|---|
| | 3.5 | | 6.5 | | 9.5 | |
| $u$, ft./sec. | $\overline{V}_b$, ft./sec. | $D_e$, ft. | $\overline{V}_b$, ft./sec. | $D_e$, ft. | $\overline{V}_b$, ft./sec. | $D_e$, ft. |
| 0.1 | 1.0 | 0.053 | 1.0 | 0.053 | 0.89 | 0.041 |
| 0.2 | 1.64 | 0.13 | 1.64 | 0.13 | 1.64 | 0.13 |
| 0.3 | 2.16 | 0.22 | 2.33 | 0.26 | 2.33 | 0.26 |
| 0.4 | 2.72 | 0.34 | 2.53 | 0.29 | 2.72 | 0.34 |
| | | (4.1 in.) | | | | |
| 0.5 | — | — | 2.67 | 0.30 | — | — |

by Davidson and Harrison (*8*) as

$$\overline{V}_b = (u - u_o) + 0.711\ (g\ D_e)^{1/2}$$

This expression was derived for single bubbles rising in an inviscid liquid, and were confirmed experimentally in incipiently fluidized beds by observing the time interval between the injection of a bubble of known volume at the base of the bed and its arrival at the surface (*9*).

Values of $D_e$ were calculated from the corresponding $\overline{V}_b$ values and both are given in Table 1 for the three columns at different gas velocities.

It may be observed that $D_e$ for the 3.5-in. column at 0.4 ft./sec. superficial gas velocity is slightly larger than the diameter of the column. This could not be true, particularly because slug flow was not noticed in any experiment. Therefore it seems that the predicted equivalent bubble diameter is somewhat larger than the actual bubble size.

## CONCLUSIONS

From the standpoint of solids distribution, an aggregatively fluidized bed consists of three axial zones: a distributor zone whose characteristics are dependent on the type of distributor used, a middle fully developed zone extending to the initial fixed bed height, and a dilute phase zone occupying the top portion of the bed and exhibiting a sharp decrease in solids concentration. Radially, solids concentration is highest at the wall and lowest at the center.

The relative void fraction distribution for each column diameter can be characterized by a single value of $N$ in the equation $\alpha/\alpha_c = S^N$ based on a mixing length model.

# PART II. STUDY OF GAS MIXING PATTERNS

In this part of the work an attempt was made to utilize the solids distribution results obtained in the first part, together with steady state gas tracer experiments, to evaluate the extent of gas back-mixing and the contacting characteristics of the fluidized system. The experiments were carried out in the 9.5-in. column and were restricted to the axially fully developed density zone.

## PREVIOUS WORK

A few gas mixing and residence time studies with tracer techniques used have been reported. Gilliland and Mason (*12, 13*) studied gas mixing and residence time distribution in two studies using 1- to 3-in. diameter beds. In the first helium tracer was generally injected at the center of the bed and gas samples were analyzed from different positions above and below the source by a gas density balance. Their results indicated that the radial tracer profiles were fairly symmetrical and that the upstream profiles indicated some backmixing. In the second study, gas residence time distribution was measured by means of purge studies in which the concentration of the exit gas was measured as a function of time after the helium tracer injection was stopped, and they found that the system approximated complete mixing.

Other investigators studied gas residence time distribution in large commercial units and in laboratory units (*1, 7, 18, 20, 24*), and their results in general confirmed the findings of Gilliland and Mason. Van Deemter (*29*), using the work of May (*24*) as a basis derived expressions for gas back-mixing and residence time distribution for a two-phase flow model, in which he showed that the gas eddy diffusivity of the dense phase, and the rate of mass transfer between the two phases, can be determined from tracer studies.

## EQUIPMENT FOR THE GAS TRACER EXPERIMENTS

Tracer experiments were performed in the 9.5-in. column. Helium was employed as the tracer gas and was injected at a fixed level of 18 in. above the porous plate distributor.

Injection and sampling tubes could be moved radially from the center to the wall of the column. Sampling tubes were located at various elevations at one inch intervals. These were 1/16-in. brass tubes whose front end was sealed and 1/32-in. holes were drilled in their walls near the front end. The holes were covered from inside with cotton filters.

Samples were analyzed with a thermal conductivity cell whose signal was recorded continuously with a Brown recorder having a full scale reading of 1 mv.

### Procedure

1. The bed was fluidized at the required superficial gas velocity.
2. The injection tube was inserted in the bed at the required radial position.
3. The tracer flow rate was adjusted to the required level. The helium injection rates used were in the range of 0.01 to 0.045% by volume of the total air flow rates.
4. Axial concentration traverses were then made by adjusting the sampling tubes in the positions required, one at a time. Samples were continually analyzed for about 10 min. so that a reproducible time-averaged response could be obtained.
5. When radial concentration traverses were required, the sampling probe was moved to the required radial positions.

## RESULTS OF THE GAS TRACER EXPERIMENTS

Complete data of the gas tracer experiments are given elsewhere (*10*). The reproducibility of the time-averaged concentration data was determined by frequent repetition, and it was found to be within ± 10%.

Data were obtained only in the fully developed region of the 9.5-in. column and therefore the zone close to the distributor and that at the top of the bed were not considered. The position of the injection tube above the distributor was fixed in all the experiments and thus the effect of tracer injection at different elevations in the bed was not studied.

### General Description of the Tracer Concentration Traverses

*Axial Profiles.* Axial tracer concentration traverses above and below the injection point and along the same longitudinal axis will be referred to as the axial profiles. Typical axial profiles are shown in Figures 9 and 10 along the center and in the neighborhood of the wall (4 in. from the center) for two gas velocities of 0.1 and 0.4 ft./sec. Tracer concentrations were all evaluated in terms of the

ratio $c/C_o$. In this ratio $C_o$ is the volumetric rate of helium divided by the volumetric air rate, and represents the composition of the completely mixed or outlet gas, whereas $c$ is the local sampled helium concentration.

Examination of the axial tracer data indicated the following observations. In the central core, downstream concentrations were high in the vicinity of the injection point and diminished rapidly to approach the completely mixed concentration within the first 4 in. Below the injection point, tracer concentrations were appreciable. They were relatively higher than the downstream concentrations at low gas velocities, but decreased gradually with increasing gas velocity.

In the wall region the upstream tracer concentrations were very substantial. The downstream concentrations were generally low and approached the completely mixed concentration within the first few inches above the injection point.

*Radial Profiles.* Typical radial concentration traverses are shown in Figures 11 and 12 for a superficial gas velocity of 0.2 ft./sec. with injection at the center and in the neighborhood of the wall (4 in. from the center). The following observations may be deduced from the radial traverses results. Radial profiles were generally skewed, and the degree of skewness was more pronounced for the profiles obtained in the wall region. Concentration peaks occurred above and below the injection point and very closely along the injection axis. The highest concentrations were generally confined within a 1- or 2-in. radius around the injection axis, whereas the rest of the concentrations approached the completely mixed gas concentrations.

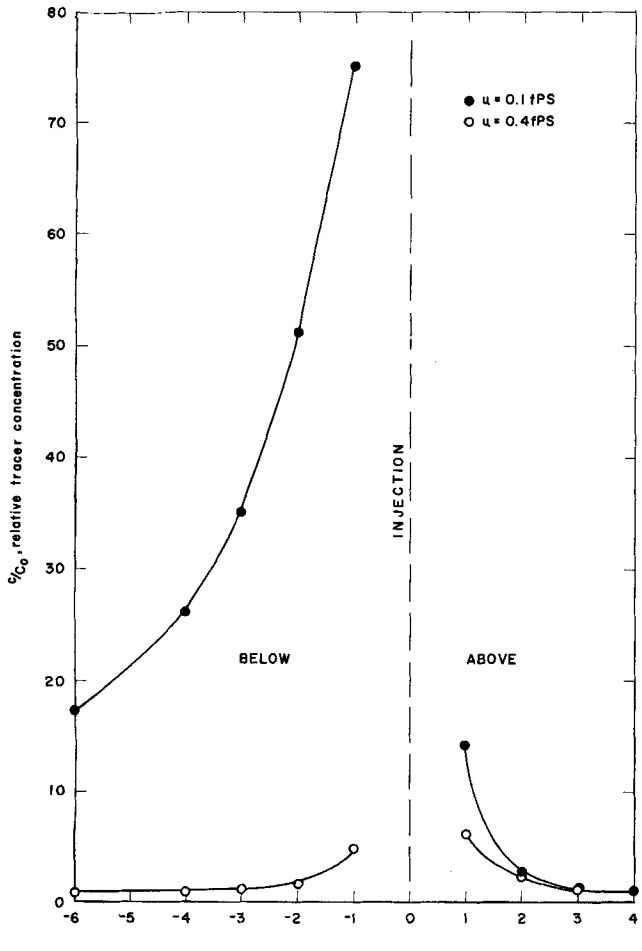


Fig. 9. Axial tracer concentrations along the center.

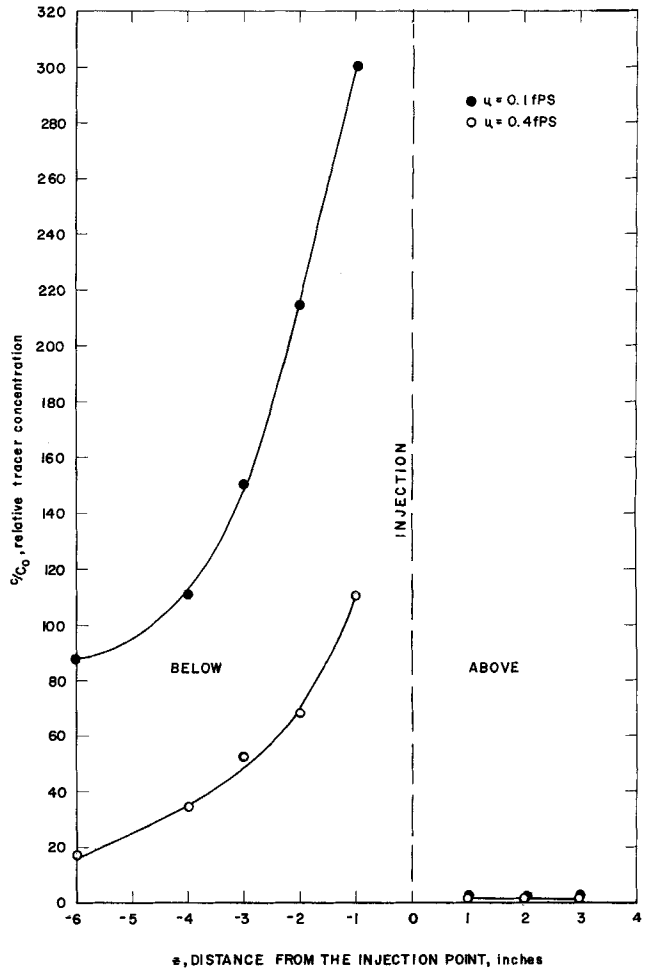


Fig. 10. Axial tracer concentrations near the wall (4 in. from center).

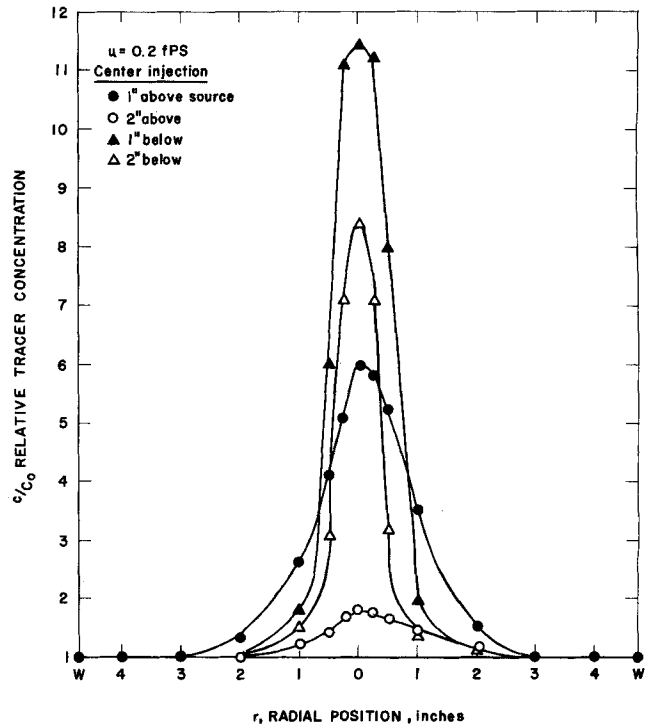


Fig. 11. Typical concentration profiles with tracer injection at the center.

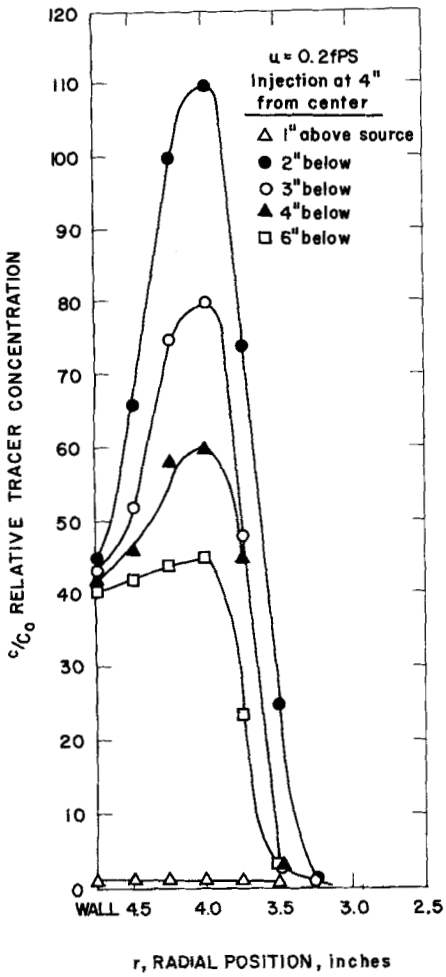


**Fig. 12. Typical radial concentration profiles with tracer injection near the wall.**

### Discussion and Interpretation of the Tracer Concentration Traverses

It is felt that measured tracer concentrations are representative of the gas in the dense phase with very little or negligible sampling from the bubble phase.

First, the vertical bubble phase velocity is much larger than that of the dense phase gas, and therefore its residence time is much smaller. Accordingly, it is most probable that samples are preferentially taken from the dense phase gas.

Second, in the preliminary experiments, a simple test was made to examine the validity of the assumption. The bed was kept at minimum fluidization with no apparent bubbles seen from the top and then the tracer was injected in single bubbles. The samples obtained above the injection point exhibited very little tracer concentration. This indicated that no sampling was made from the bubble phase, which in this case presumably contained all the tracer injected.

*Tracer Transfer at the Injection Point.* The mode of tracer transfer to the dense phase at the injection point is quite similar in nature to that occurring at the bed distributor which has been postulated by several investigators to account for most of the gas exchange between the dense and bubble phases. Consequently, examination of the extent of tracer transfer at the injection point should yield some information in this respect.

The fraction of the tracer injected into each phase would be ideally dependent upon the volume fraction occupied by each phase. Therefore, near the column wall where very little or no bubbles exist, most of the tracer will be injected directly into the dense phase. Around the center, on the other hand, the tracer would be distributed between the two phases, and the amount injected into the dense phase would generally decrease as the gas velocity is increased. It may be also noted that the fraction transferred to the dense phase will increase if a degree of defluidization occurs in that phase, which has been actually observed to occur above obstruction surfaces inserted into a fluidized bed (*14*).

An indication of the fraction of the tracer injected into the dense phase can be obtained by extrapolating the upstream tracer concentrations to the injection point. Some values of the tracer concentration at the injection point calculated in this way are given in Table 2. These values and their trend are consistent with what was expected from the known volume fractions as indicated in the previous paragraph.

*Tracer Distribution in the Wall Region.* The wall region is characterized by a low bubble void fraction and consists mostly of heavy particle aggregates moving predominantly downward. Consequently, one would expect appreciable tracer concentration below the injection point. On the other hand, the concentrations above the injection point will generally be low, and will depend upon the amount of the tracer injected into the bubbles, bubble frequency, and the rate of mass transfer between the two phases. The results are in close agreement with these expectations.

*Tracer Distribution in the Central Core.* The central core of the bed is characterized by a large number of bubbles, and a dense phase with a net upward velocity consisting of aggregates whose size and lifetime are dependent on the bubble frequency. According to this picture, high tracer concentrations prevail above the injection point, whereas much lower concentrations are expected in the upstream side.

Examination of the tracer concentration profiles indicated some disagreement with these expectations. This is particularly so at low gas velocities where the tracer concentrations below the source were higher than those above it. This peculiar distribution indicates the existence of large falling aggregates at low gas velocities. These falling aggregates tend to trap the tracer gas and drag it downward with them. This leads to extensive back-mixing. At higher velocities, these aggregates seem to become smaller in size and shorter in lifetime because of the more frequent passage of rising bubbles.

The occurrence of high concentrations and the appearance of large peaks in the radial concentration profiles below the injection point prove that back-mixing occurs both by tracer transfer from the center to the wall, where it is carried below the injection point, as is generally believed, and by local downflow at each point in the bed. Accordingly, then, there must exist well-organized circulation patterns caused by bubbles passing. Therefore the assumption that back-mixing is caused by random motion is a questionable one.

Since local downflow does occur, and since the net

Table 2. $c/C_0$ Relative Tracer Concentration at the Injection Point

(Extrapolated)

| | Injection position | | |
|---|---|---|---|
| $u$, ft./sec. | Center | 2 in. from center | 4 in. from center |
| 0.1 | 110 | 240 | 455 |
| 0.2 | 22.5 | 115 | 320 |
| 0.3 | 10.3 | 24.5 | 200 |
| 0.4 | 3.1 | 30.4 | 190 |

dense gas velocity in the central core is upward, then there should be a coexistent upflow of small aggregates associated with the bubbles and travelling at high vertical velocities. These observations combined seem to indicate that sampling was made preferentially from the gas entrained in the falling aggregates. This conclusion is supported to a large extent by the recent findings of flow patterns associated with a rising bubble (*26, 27, 30*), which indicate that solid particles and entrained gas flow downward in streamlines around the bubble, while a spout of small aggregates is drifted into its wake. According to this picture, sampling should be mostly representative of the downfalling aggregates, since the upward drift of the small aggregates gas following the wake of the bubble will tend to bypass the sampler and be drifted into the bubble.

Such an explanation clarifies and accounts for the peculiar tracer distribution especially at the low velocities. Thus, the downfalling aggregates will drag a large fraction of the tracer leading to the appearance of appreciable concentration below the source. Above the injection point, the downfalling gas will be coming from the top of the bed with a tracer concentration equal to that at the outlet or the completely mixed concentration. Any increase in its concentration while approaching the injection point will result from mixing with the upward drift spout and by mass transfer with the rising bubbles. This explanation accounts for the relatively low downstream concentrations and their rapid approach to the completely mixed concentration.

## FLUIDIZED BED MODEL

Several models have been proposed in the literature to characterize the flow behavior of fluid beds for the ultimate purpose of predicting the extent of heterogeneous reactions. All these models are based essentially on the two-phase flow concept which regards the fluidized system as consisting of a dense phase, agitated by fast rising bubbles which exchange gas with the dense phase as they rise. The degree of complexity of these models varies considerably, depending on the number of parameters included.

The most complicated model, by Van Deemter, does not account for axial and radial variations in phase properties. The model described here is an extension of Van Deemter's model taking into consideration axial and radial variations.

It assumes that the fluidized bed is composed of two phases; that the dispersed phase gas travels in plug flow; that the continuous exchange of gas between the two phases can be characterized by means of a mass transfer coefficient; that the continuous disintegration and coalescence of particle aggregates impose a random motion on the dense phase gas, which can be described with the aid of an eddy diffusivity; and that radial and angular eddy diffusion or mixing effects are negligible compared to axial diffusion. The basic differential equations are the same as used by Van Deemter (*29*) and the solution is of the same form. The boundary conditions $dc/dz = 0$ and $c = C = C_o$ were found experimentally to hold as the top of the bed was approached.

Then if the dense phase is taken as that portion composed of the large falling aggregates, and the dispersed phase as the bubbles and the attached upflowing small aggregates, the physical picture will bear a closer analogy to the actual behavior of the fluidized bed as indicated by the tracer experiments.

Experimental measurements of the time-averaged phase concentrations conducted in this work indicated the existence of a fully developed region about one bed diameter above the distributor. It was assumed that the velocity profiles are also fully developed in this region.

It is not possible to evaluate the parameters of the model with confidence. Nevertheless, utilizing the recent findings of bubble studies, we made calculations to estimate them at the lowest gas velocity used (0.1 ft./sec.). The method of calculation consisted essentially of estimating the model's six parameters ($f$, $F$, $V$, $v$, $E$, and $k$) in the following way:

1. The volume fraction occupied by the downfalling aggregates gas $f$ and that occupied by the dispersed phase gas (bubbles and the gas in the attached solids) $F$ were estimated from the solids distribution measurements by assuming that the fraction of the particulate phase attached with the bubbles to form the dispersed phase occupies a volume fraction equal to 0.7 of the time-averaged bubble volume fraction. This assumption is based on the recent finding from bubble studies indicating that the volume of the spout drifted in the wake of the bubble is about 0.7 of the bubble volume.
2. The velocity of the dispersed phase gas $V$ was estimated by assuming that it is equal to the bubble velocity, and that its radial profile follows the same shape as that of the time-averaged bubble volume fraction.
3. The remaining three parameters, $v$ the velocity of the falling aggregates, $E$ the eddy diffusivity of the falling aggregates, and $k$ the mass transfer coefficient between phases, were then estimated at the center. This was done by assuming an approximate boundary condition at the injection point, stating that all the tracer is injected into the falling aggregates, and fitting the axial tracer results to the mathematical solutions.
4. From the calculated value of the velocity of the falling aggregates at the center, the net velocity at the center of the gas in all the particulate phase was calculated by assuming that the gas in the solids attached with the dispersed phase travels upward at a velocity equal to that of the bubbles. The net velocities at locations other than the center were then estimated by assuming that its radial profile follows the same shape as that of the time-averaged bubble volume fraction, and the velocity of the falling aggregate gas at various radial positions could therefore be calculated.
5. The estimated eddy diffusivity at the center was found to be small and of minor effect on back-mixing compared with that of the velocity of the downfalling aggregates, and it was therefore neglected at all radial positions other than the center.
6. The mass transfer coefficient $k$ at various radial positions was finally calculated by fitting the upstream tracer concentration results to the mathematical solutions of the model.

The final estimated results of the model parameters are given in Table 3. It should be pointed out that these results only illustrate the order of magnitude of the different parameters.

Table 3. Summary of the Calculated Results of the Model Parameters at a Superficial Gas Velocity of 0.1 Ft./Sec.

| | Radial position, in. from center | | | | |
|---|---|---|---|---|---|
| | 0 | 1 | 2 | 3 | 4 |
| $\alpha$ | 0.15 | 0.14 | 0.12 | 0.10 | 0.06 |
| $F$ | 0.225 | 0.21 | 0.18 | 0.15 | 0.09 |
| $f$ | 0.525 | 0.54 | 0.565 | 0.59 | 0.64 |
| $V$ | 1.78 | 1.7 | 1.46 | 1.07 | 0.51 |
| $v$ | 0.107 | 0.10 | 0.077 | 0.038 | −0.015 |
| $\overline{v}$ | −0.05 | −0.035 | −0.019 | −0.027 | −0.05 |
| $k$ | 0.18 | 0.13 | 0.07 | 0.12 | 0.58 |
| $E$ | 0.0026 | — | — | — | — |

The following remarks are in order:

1. Even though the estimated value of the eddy diffusivity at the center is very small compared to values reported in the literatures it is about twenty times the order of magnitude of the gas molecular diffusivity.

2. The estimated values of the net velocity of all the particulate phase gas indicate that, although local downflow occurs everywhere in the bed, the net value in the central region is positive (upward in direction) as it should.

3. The mass transfer coefficient $k$ provides some idea about the effectiveness of contact between phases, and its magnitude is very important from the standpoint of heterogeneous reactions. Overall exchange coefficients between phases in fluidized beds have been reported in literature from chemical reaction studies (*15, 23, 28*). These can be related to the mass transfer coefficients estimated here, but they are not directly comparable, since the operating conditions (specifically from the standpoint of column diameter) are different. It was interesting to note that the values of $k$ calculated from Gomezplata's data (*15*) are of the same order of magnitude as the ones estimated in this study.

#### Comparison with Previous Tracer Studies

Gilliland and Mason (*15*) were the only investigators who reported a steady state gas tracer study using the point source technique. The results of this work are not directly comparable with their results, since they used small-diameter beds (1 and 3 in. I.D.) and injected large amounts of tracer (averaging about 10% of the total gas flow), in contrast with the trace amounts employed in this work (maximum injection rate of 0.045%). The large tracer rates used in their study probably disturbed the flow behavior of the bed, and the tracer was probably channeling in the injection region.

The downstream concentrations reported in their work were higher than those of this study. Their upstream concentrations were lower and did not exhibit any peaks. Their results were correlated with a single parameter, the eddy diffusivity of the gas phase, and they did not account in any way for the mass transfer between phases.

## CONCLUSIONS

Gas back-mixing in a fluidized bed can be appreciable and is caused primarily by local solids downflow at every point in the bed. A model based on two phases, one composed of large falling aggregates and the other of bubbles with attached upflowing aggregates, is consistent with the experimental observations. Estimated parameters for the model at low gas velocities were found to be reasonable.


## ACKNOWLEDGMENT

Computer time was supported through the facilities of the Computer Science Center of the University of Maryland under NASA Grant 398. The authors are also indebted to the Nuclear Reactor Group for the use of their facilities.


## NOTATION

$c$ and $C$ = tracer concentrations of the dense and dispersed phase gases, respectively
$C_o$ = completely mixed or outlet gas concentration
$D$ = time-averaged point solids concentration
$D'$ = fluctuating density component
$D_b$ = solids settled bulk density
$D_m$ = solids mean path concentration
$D_e$ = equivalent bubble diameter
$E$ = axial eddy diffusivity of the dense phase gas
$f, F$ = volume fractions occupied by the dense and dispersed phase gases, respectively
$g$ = gravitational constant
$k$ = mass transfer coefficient
$k_1$ = constant
$K$ = constant
$L$ = absorber thickness
$l_D$ = density mixing length
$N$ = power law exponent
$r$ = radial position
$R$ = column radius
$s$ = dimensionless distance from the wall
$u$ = superficial gas velocity
$u_o$ = minimum fluidization velocity
$\overline{V}_b$ = average rate of bubble rise
$V$ = dispersed phase gas velocity
$v$ = dense phase gas velocity
$z$ = axial position from the injection point
$\alpha$ = time-averaged bubble volume fraction
$\alpha_c$ = time-averaged bubble volume fraction at the center
$\overline{\alpha}$ = area-averaged bubble volume fraction

## LITERATURE CITED


1. Askins, J. W., G. P. Hinds, and F. Kunreuther, *Chem. Eng. Progr.*, **47**, 401 (1951).
2. Bakker, P. J., and P. M. Heertjes, *Brit. Chem. Eng.*, **4**, 524 (1959).
3. ———, *Chem. Eng. Sci.*, **12**, 260 (1960).
4. Bankoff, S. G., *J. Heat Transfer*, **82**, 265 (1960).
5. Bartholomew, R. N., and R. M. Casagrande, *Ind. Eng. Chem.*, **49**, 428 (1957).
6. Baumgarten, P. K., and R. L. Pigford, *A.I.Ch.E. J.*, **6**, 115 (1960).
7. Danckwerts, P. V., J. W. Jenkins, and G. Place, *Chem. Eng. Sci.*, **3**, 26 (1954).
8. Davidson, J. F., and D. Harrison, "Fluidized Particles," Cambridge Univ. Press (1963).
9. Davidson, J. F., R. C. Paul, M. J. S. Smith, and H. A. Duxbury, *Trans. Inst. Chem. Eng.*, **37**, 323 (1959).
10. El Halwagi, M. M., Ph.D. thesis, Univ. Maryland, College Park (1965).
11. Fan, L. T., C. H. Lee, and R. C. Bailie, *A.I.Ch.E. J.*, **8**, 239 (1962).
12. Gilliland, E. R., and E. A. Mason, *Ind. Eng. Chem.*, **41**, 1191 (1949).
13. *Ibid.*, **44**, 218 (1952).
14. Glass, D. H., and D. Harrison, *Chem. Eng. Sci.*, **19**, 1001 (1964).
15. Gomezplata, Albert, and W. W. Shuster, *A.I.Ch.E. J.*, **6**, 454 (1960).
16. Grek, F. Z., and V. N. Kisel'nikov, *Intern. Chem. Eng.*, **4**, No. 2, 263 (1964).
17. Grohse, E. W., *A.I.Ch.E. J.*, **1**, No. 3, 358 (1955).
18. Handlos, A. E., R. W. Kunstman, and D. O. Schissler, *Ind. Eng. Chem.*, **49**, 25 (1957).
19. Hunt, R. H., W. R. Biles, and C. O. Reed, *Petrol. Refiner*, **36**, No. 4, 179 (1957).
20. Huntley, A. R., *Ind. Eng. Chem.*, **53**, 381 (1961).
21. Levy, S., *J. Heat Transfer*, **85**, 137 (1962).
22. Matheson, G. L., W. A. Herbst, and P. H. Holt, *Ind. Eng. Chem.*, **41**, 1099 (1949).
23. Mathis, J. F., and C. C. Watson, *A.I.Ch.E. J.*, **2**, 518 (1956).
24. May, W. G., *Chem. Eng. Progr.*, **55**, 49 (1959).
25. Rowe, P. N., *Chem. Eng. Progr. Symp. Ser. No. 38*, **58**, 42 (1962).
26. Rowe, P. N., and B. A. Partridge, *Chem. Eng. Sci.*, **18**, 511 (1963).
27. ———, and E. Lyall, *Chem. Eng. Sci.*, **19**, 973 (1964).
28. Shen, C. Y., and H. F. Johnstone, *A.I.Ch.E. J.*, **1**, 349 (1955).
29. Van Deemter, J. J., *Chem. Eng. Sci.*, **13**, 143 (1961).
30. Wace, P. F., and S. J. Burnett, *Trans. Inst. Chem. Eng.*, **39**, 168 (1961).



*Manuscript received April 7, 1966; revision received October 10, 1966; paper accepted October 10, 1966.*